

Templated Synthesis, Postsynthetic Metal Exchange, and Properties of a Porphyrin-Encapsulating Metal–Organic Material

Zhenjie Zhang,[†] Linping Zhang,[†] Lukasz Wojtas,[†] Patrick Nugent,[†] Mohamed Eddaoudi,^{†,‡} and Michael J. Zaworotko^{*,†}

[†]Department of Chemistry, University of South Florida, 4202 East Fowler Avenue, CHE205, Tampa, Florida 33620, United States

[‡]Chemical Science, 4700 King Abdullah University of Science and Technology, Thuwal 23955-6900, Kingdom of Saudi Arabia

S Supporting Information

ABSTRACT: Reaction of biphenyl-3,4',5-tricarboxylate (H₃BPT) and CdCl₂ in the presence of *meso*-tetra(*N*-methyl-4-pyridyl)porphine tetratosylate (TMPyP) afforded **porph@MOM-10**, a microporous metal–organic material containing CdTMPyP cations encapsulated in an anionic Cd(II) carboxylate framework, [Cd₆(BPT)₄Cl₄(H₂O)₄]. **porph@MOM-10** is a versatile platform that undergoes exchange to serve as the parent of a series of **porph@MOMs** that exhibit permanent porosity and heterogeneous catalytic activity.

The extra-large surface area exhibited by certain metal–organic materials (MOMs) affords them the opportunity to impact technologies for gas storage,^{1–3} gas separation,^{4–6} luminescence,⁷ magnetism,^{8,9} catalysis,^{10,11} and other applications.^{12,13} An important feature of MOMs is that they exhibit diversity of scale and composition that is more extensive than that of inorganic porous materials such as zeolitic aluminosilicates and aluminophosphates. In particular, MOMs can be deliberately designed by selecting geometrically compatible nodes (metals or metal clusters) and linkers (organic ligands). Moreover, the modular components of MOMs can be preselected or altered by postsynthetic modification (PSM) to tune the physicochemical and chemical properties of the resulting MOMs.^{14,15} The versatility of MOMs is exemplified by the way that porphyrins, which are widely used as catalysts and dyes,¹⁶ can be incorporated into MOMs,¹⁷ usually as custom-designed porphyrin ligands.¹⁸ Porphyrin-encapsulating MOMs (**porph@MOMs**) can exist if MOMs contain cages with the requisite size and shape but are limited to three examples: a discrete pillared coordination box (**porph@MOM-1**),¹⁹ a zeolitic metal–organic framework (**porph@MOM-2**),²¹ and HKUST-1 (**porph@MOM-3**).²⁰ We have addressed the dearth of **porph@MOMs** by employing porphyrins as structure-directing agents (SDAs) to template a series of six **porph@MOMs** in which a novel framework self-assembles around porphyrin molecules, trapping them in a “ship-in-a-bottle” fashion.²² The availability of **porph@MOMs** via porphyrin-templated synthesis affords an opportunity to address PSM of the encapsulated metalloporphyrin moieties in order to study their impact upon properties such as catalysis, gas sorption, and luminescence.

In this contribution, we demonstrate that **porph@MOM-10**, a MOM that contains CdTMPyP cations [TMPyP = *meso*-

tetra(*N*-methyl-4-pyridyl)porphine tetratosylate] encapsulated in a Cd(II) carboxylate framework, can be subjected to PSM of the metal moieties. Retention of the parent framework during PSM of a porous Cd metal–organic framework (MOF) with Pb^{23–25} has already been observed, and it has long been known that smaller divalent cations can replace larger divalent ions in metalloporphyrins.²⁶ A Cd(II)-based **porph@MOM** such as **porph@MOM-10** therefore represents an ideal candidate for PSM, and as revealed herein, it readily undergoes single-crystal-to-single-crystal PSM.

Reaction of biphenyl-3,4',5-tricarboxylate (H₃BPT),²⁷ CdCl₂, and TMPyP in *N,N*-dimethylformamide/H₂O afforded dark prismatic crystals of [Cd₆(BPT)₄Cl₄(H₂O)₄]·[C₄₄H₃₆N₈CdCl]·[H₃O]·[solvent] (**porph@MOM-10**) that adopted the tetragonal space group *P4/n* with *a* = *b* = 28.9318(4) Å and *c* = 10.3646(3) Å. The as-synthesized crystals exhibit macroscale semiregular hexagonal or square channels along the [110] direction (Figure S1 in the Supporting Information). Single-crystal X-ray determination (SCXRD) revealed that **porph@MOM-10** is an anionic framework with open channels that contain TMPyP and H₃O⁺ counterions.²³ The same reaction conducted in the absence of TMPyP afforded colorless block crystals of a different product (Figure S2). Figure 1 reveals that the framework of **porph@MOM-10** contains two independent Cd(II) cations (Cd1 and Cd2), one crystallography independent BPT ligand, and one crystallographically ordered CdTMPyP cation. Cd2 adopts a distorted octahedral geometry via coordination to four carboxylate oxygen atoms, an aqua ligand, and a μ₂-chloride anion, whereas Cd1 possesses distorted octahedral geometry through four carboxylate oxygen atoms and two μ₂-chloride anions. The Cd–O bond distances range from 2.205(5) to 2.392(5) Å, and the Cd–Cl bond distances lie between 2.560(2) and 2.682(7) Å, both ranges being consistent with expected values.²⁸ Cd1 and Cd2 thereby form a 6-connected trimetallic molecular building block (MBB), [Cd₃(Cl)₂(COO)₆]^{2–}, that does not exist in the Cambridge Structural Database (CSD).²⁹ These MBBs are linked by 3-connected BPT ligands to form a 3,6-connected network (Figure S3) with the Schläfli symbol {4-6²}₂{4²-6¹⁰-8³}. Projecting the structure along the *c* axis (Figure 1 left) reveals that there is a 1:1 ratio of two types of square channels: (A)

Received: October 13, 2011

Published: December 20, 2011

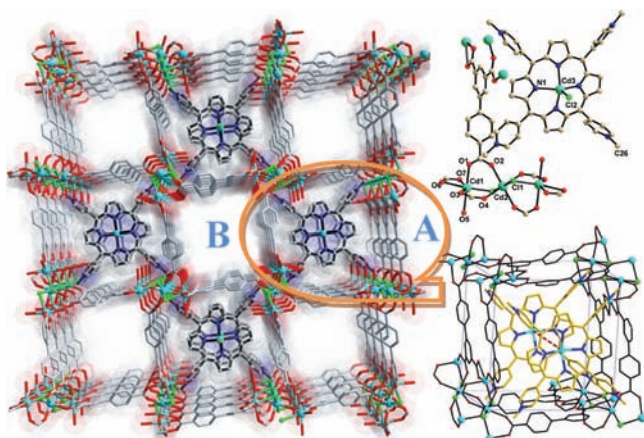


Figure 1. (left) Projection of the structure of **porph@MOM-10** along the *c* axis. (upper right) Components of the framework and **CdTMPyP** cations in **porph@MOM-10**. (lower right) Illustration of **CdTMPyP** cations trapped in cuboid boxes in **porph@MOM-10**.

$\sim 12.6 \text{ \AA} \times 12.6 \text{ \AA}$; (B) $\sim 11.9 \text{ \AA} \times 11.9 \text{ \AA}$ (after subtracting van der Waals radii). **CdTMPyP** cations stack in channels A separated by 10.3 \AA , whereas channels B are occupied by solvent molecules. Figure 1 (lower right) reveals that **CdTMPyP** cations are encapsulated in a cuboid nanoscale box. A tight fit is seen as follows: $\pi \cdots \pi$ interactions (3.3 and 3.2 \AA) between the porphyrin arms (pyridyl groups) and phenyl groups of adjacent BPT ligands; C–H \cdots O interactions between the methyl groups of **CdTMPyP** and μ_2 -connected chlorides (3.65 \AA , C–H \cdots Cl = 170°); and electrostatic interactions between the anionic framework and cationic porphyrin molecules. The cuboid box has four open faces with $\sim 7 \text{ \AA} \times 10 \text{ \AA}$ windows that are exposed to channel B, thereby facilitating access to the porphyrin moiety. Removal of all solvent molecules would create an accessible free volume of $\sim 4484 \text{ \AA}^3$, or 52% of the volume of the unit cell (PLATON).³⁰

Cd^{2+} cations lie out of the **TMPyP** plane: ΔC_β , the average deviation of β -carbon atoms from the porphyrin plane (Figure S4), is 0.23 \AA , and the Cd–N bond distances are $2.256(3) \text{ \AA}$.³¹ Crystals of **porph@MOM-10** were immersed in a methanol solution of MnCl_2 that was refreshed every 24 h, and the resulting exchange process was monitored by UV–vis spectroscopy, which showed that conversion of **CdTMPyP** to **MnTMPyP** was complete within 1 week. Atomic absorption (AA) revealed that the Cd framework was almost completely exchanged by Mn (Figure S5) after 1 month. The resulting crystals retained their crystallinity (Figure S6), as confirmed by SCXRD of the resulting compound, **Mnporph@MOM-10-Mn**, of composition $[\text{Mn}(\text{II})_6(\text{BPT})_4\text{Cl}_4(\text{CH}_3\text{OH})_4] \cdot [\text{C}_{44}\text{H}_{36}\text{N}_8\text{Mn}(\text{III})] \cdot \text{Cl} \cdot [\text{solvent}]$. The unit cell parameters of **Mnporph@MOM-10-Mn**, $a = b = 28.505(1)$ and $c = 10.371(1)$, are reduced, presumably because of shorter Mn–O (average 2.179 \AA) and Mn–Cl [$2.464(1)$ and $2.561(1) \text{ \AA}$] distances. Mn3 is located in the plane of the porphyrin with $\Delta C_\beta = 0$ and Mn–N = $2.015(3) \text{ \AA}$ (Figure S7). A CSD survey revealed that Mn(II)–O and Mn(III)–N distances average $\sim 2.16 \text{ \AA}$ and 2.00 \AA , respectively,^{32,33} indicating that Mn1 and Mn2 are +2 cations whereas Mn3 is a +3 cation. The UV–vis spectrum of commercial Mn(III)-**TMPyP** correlates well with that of the porphyrin moiety in **Mnporph@MOM-10-Mn** (Figure S8). When a solution of CuCl_2 was contacted with **porph@MOM-10** for ~ 3 days,

CdTMPyP ($\lambda_{\text{max}} = 426.4 \text{ nm}$) was transformed to **CuTMPyP** ($\lambda_{\text{max}} = 430.0 \text{ nm}$) (Figure 2 right), but the Cd framework was

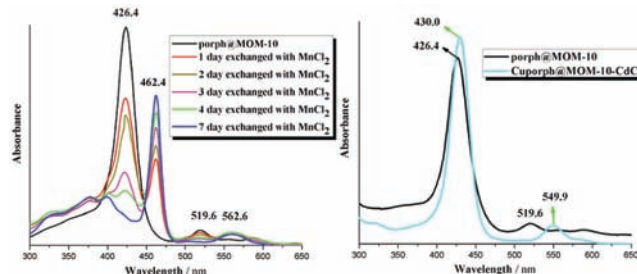


Figure 2. (left) Solution-state UV–vis spectra of **porph@MOM-10** immersed in MnCl_2 solution at different times, revealing that the Soret band of **CdTMPyP** ($\lambda_{\text{max}} = 426.4 \text{ nm}$) decreased as the Soret band of **MnTMPyP** ($\lambda_{\text{max}} = 462.4 \text{ nm}$) increased. (right) UV–vis spectra of **Cuporph@MOM-10-CdCu** and **porph@MOM-10** in water.

only partly exchanged with Cu ($\sim 76\%$ had been exchanged after 1 month). SCXRD revealed that the resulting compound, **Cuporph@MOM-10-CdCu**, has the approximate formula $[\text{Cu}_4\text{Cd}_2(\text{BPT})_4\text{Cl}_4(\text{CH}_3\text{OH})_4] \cdot [\text{C}_{44}\text{H}_{36}\text{N}_8\text{Cu}] \cdot [\text{solvent}]$ and exhibits unit cell parameters $a = b = 29.2846(9)$ and $c = 9.9941(4) \text{ \AA}$. Cd1 is partially exchanged by Cu, whereas Cd2 is completely exchanged [the Cu–O bond lengths of $1.917(6)$ – $1.995(6) \text{ \AA}$ are consistent with previously reported Cu(II)–O bond lengths³⁴]. Cu3 is located in the plane of the porphyrin, with $\Delta C_\beta = 0$ and Cu–N = $1.975(6) \text{ \AA}$ (Figure S10). Attempts to prepare these **porph@MOMs** directly by reaction of Mn or Cu salts with H_3BPT were unsuccessful.

Berezin reported that the metal exchange process of Cd porphyrins is kinetically controlled.³¹ Our observations indicate that exchange of the framework Cd2 cations is presumably facilitated by the presence of a relatively labile aqua ligand. That Cd1 is completely exchanged by Mn(II) but only partly exchanged in the case of Cu(II) might be attributed to the lability of high-spin d^{10} and d^9 metals and the relative inertness of low-spin d^5 metals such as Mn(II).

Thermogravimetric analysis (Figures S11–S13) showed that **porph@MOM-10**, **Mnporph@MOM-10-Mn**, and **Cuporph@MOM-10-CdCu** exhibit similar thermal stability with ~ 10.0 , 17.8 , and 8.3% weight loss, respectively, below $100 \text{ }^\circ\text{C}$ and stability to ~ 300 , 370 , and $270 \text{ }^\circ\text{C}$, respectively. To evaluate the porosities of these materials, N_2 and H_2 adsorption studies were performed (Figure 3). **Porph@MOM-10** and its metal-exchanged analogues were subjected to methanol exchange and activated at $60 \text{ }^\circ\text{C}$ for 10 h. The N_2 adsorption isotherms at 77 K represent type-I sorption behavior characteristic of microporosity. **Porph@MOM-10**, **Mnporph@MOM-10-Mn**, and **Cuporph@MOM-10-CdCu** adsorb 311 , 298 , and $102 \text{ cm}^3/\text{g}$ of N_2 , respectively (77 K , $P/P_0 = 0.95$). These correspond to Brunauer–Emmett–Teller (Langmuir) surface areas of 1158 (1309), 1140 (1282), and $290 \text{ m}^2/\text{g}$ ($332 \text{ m}^2/\text{g}$), respectively. A pore size distribution analysis of these samples revealed a narrow distribution of micropores centered at $\sim 12 \text{ \AA}$ (Figures S14–S16), in excellent agreement with the SCXRD data. The samples after N_2 adsorption were amorphous.³⁵ H_2 adsorption isotherms (Figure 3b,c) revealed that **porph@MOM-10**, **Mnporph@MOM-10-Mn**, and **Cuporph@MOM-10-CdCu** adsorb $144 \text{ cm}^3/\text{g}$ ($1.30 \text{ wt } \%$) at 77 K and $114 \text{ cm}^3/\text{g}$ ($1.02 \text{ wt } \%$) at 87 K , $175 \text{ cm}^3/\text{g}$ ($1.58 \text{ wt } \%$) at 77 K and $127 \text{ cm}^3/\text{g}$ ($1.14 \text{ wt } \%$) at 87 K , and $47 \text{ cm}^3/\text{g}$ ($0.42 \text{ wt } \%$) at 77 K

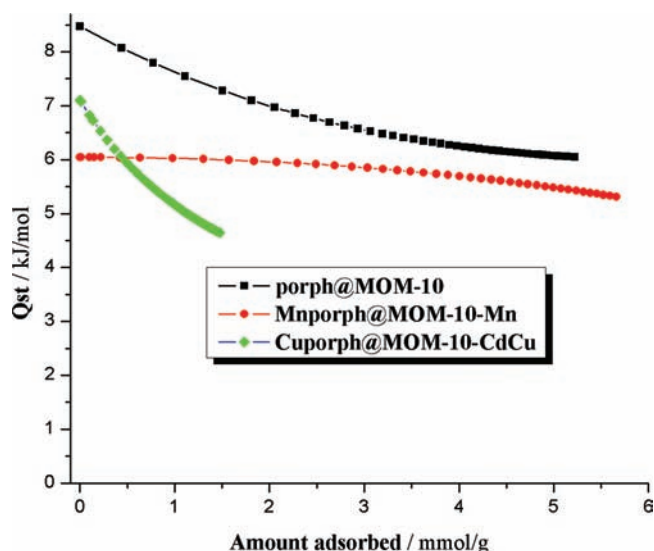


Figure 3. (a) N₂ adsorption isotherms at 77 K, (b, c) H₂ adsorption isotherms at (b) 77 and (c) 87 K, and (d) isosteric heats of adsorption for porph@MOM-10, Mnporph@MOM-10-Mn, and Cuporph@MOM-10-CdCu.

and 32 cm³/g (0.29 wt %) at 87 K, respectively, at 1 atm, with initial isosteric heats of adsorption (Q_{st}) of 8.5, 6.0 and 7.1 kJ/mol, respectively (Figure 3d). The Q_{st} of porph@MOM-10 is higher than those of HKUST-1 (Q_{st} = 6.8 kJ/mol),³⁶ MOF-5 (Q_{st} = 4.8 kJ/mol),³⁷ and MIL-100 (Q_{st} = 6.3 kJ/mol),³⁸ which may be ascribed to the binding affinity of H₂ for the open metal sites or the metalloporphyrins in porph@MOM-10.

The catalytic activities of these materials for the epoxidation of *trans*-stilbene (cross-section of 4.2 Å × 11.4 Å), a classic reaction catalyzed by metalloporphyrins,³⁹ were evaluated. In a typical reaction, samples were activated using the same procedure used for N₂ adsorption studies, and then 10.0 mg of porph@MOM was placed in a solution containing 1.0 mmol of *trans*-stilbene, 1.5 mmol of *tert*-butyl hydroperoxide (t-BuOOH), and 40.0 μL of 1,2-dichlorobenzene (internal standard) in 5.0 mL of MeCN. Reactions were conducted at 60 °C for 12 h and monitored in real time by GC–MS. As revealed by Figure 4, porph@MOM-10 exhibited only ~7%

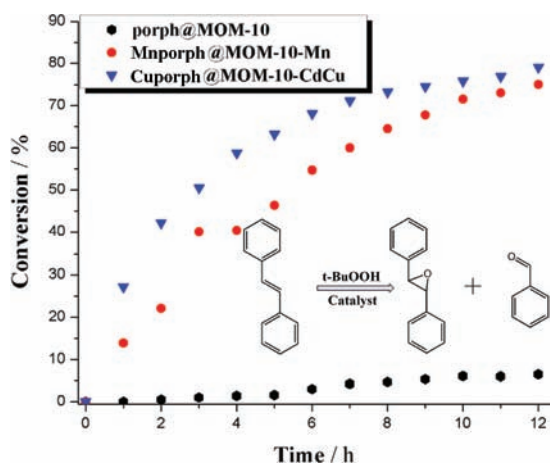


Figure 4. Comparison of the catalytic activities of porph@MOM-10, Mnporph@MOM-10-Mn, and Cuporph@MOM-10-CdCu for the epoxidation of *trans*-stilbene.

conversion, which compares closely to the <10% conversion obtained in a blank reaction without catalyst. Mnporph@MOM-10-Mn exhibited 75% conversion under the same conditions [turnover number (TON) = 178], which is similar to the 85% conversion we obtained for an equivalent molar amount of commercial Mn(III)TMPyP in solution (Table S1). Stilbene oxide and benzaldehyde were the major products (56 and 21% yield, respectively). Cuporph@MOM-11-CdCu afforded a conversion of 79% (TON = 182) with 61 and 19% yields of stilbene oxide and benzaldehyde, respectively. The filtrate after these reactions was recycled, and even after six 12 h cycles we observed *trans*-stilbene conversions of >61% for Mnporph@MOM-10-Mn (Figure S17) and >69% for Cuporph@MOM-10-CdCu (Figure S18).

In conclusion, TMPyP served as a template for the generation of porph@MOM-10, a Cd(II)-based porph@MOM that undergoes PSM by Mn(II) and Cu(II) via single-crystal-to-single-crystal processes. The resulting porph@MOMs are permanently porous, and the Mn- and Cu-exchanged variants exhibit catalytic activity for the epoxidation of *trans*-stilbene by t-BuOOH.

■ ASSOCIATED CONTENT

📄 Supporting Information

TGA, PXRD, and UV data; pore size distributions; crystal supporting figures; catalysis details; and crystallographic data (CIF). This material is available free of charge via the Internet at <http://pubs.acs.org>.

■ AUTHOR INFORMATION

Corresponding Author

xtal@usf.edu

■ ACKNOWLEDGMENTS

This publication is based on work supported by Award FIC/2010/06 made by King Abdullah University of Science and Technology (KAUST).

■ REFERENCES

- (1) Farha, O. K.; Yazaydn, A. Ö.; Eryazici, I.; Malliakas, C. D.; Hauser, B. G.; Kanatzidis, M. G.; Nguyen, S. T.; Snurr, R. Q.; Hupp, J. T. *Nat. Chem.* **2010**, *2*, 944.
- (2) Yang, S. H.; Lin, X.; Blake, A. J.; Walker, G. S.; Hubberstey, P.; Champness, N. R.; Schroder, M. *Nat. Chem.* **2009**, *1*, 487.
- (3) Sumida, K.; Brown, C. M.; Herm, Z. R.; Chavan, S.; Bordiga, S.; Long, J. R. *Chem. Commun.* **2011**, *47*, 1157.
- (4) Zhang, J.; Wu, H.; Emge, T. J.; Li, J. *Chem. Commun.* **2010**, *46*, 9152.
- (5) Zou, R.; Abdel-Fattah, A. I.; Xu, H.; Zhao, Y.; Hickmott, D. D. *CrystEngComm* **2010**, *12*, 1337.
- (6) Xue, M.; Zhang, Z.; Xiang, S.; Jin, Z.; Liang, C.; Zhu, G.-S.; Qiu, S.-L.; Chen, B. *J. Mater. Chem.* **2010**, *20*, 3984.
- (7) Allendorf, M. D.; Bauer, C. A.; Bhakta, R. K.; Houk, R. J. T. *Chem. Soc. Rev.* **2009**, *38*, 1330.
- (8) Kurmoo, M. *Chem. Soc. Rev.* **2009**, *38*, 1353.
- (9) Weng, D.-F.; Wang, Z.-M.; Gao, S. *Chem. Soc. Rev.* **2011**, *40*, 3157.
- (10) Lee, J.; Farha, O. K.; Roberts, J.; Scheidt, K. A.; Nguyen, S. T.; Hupp, J. T. *Chem. Soc. Rev.* **2009**, *38*, 1450.
- (11) Ma, L.; Abney, C.; Lin, W. *Chem. Soc. Rev.* **2009**, *38*, 1248.
- (12) Harbuzaru, B. V.; Corm, A.; Rey, F.; Jordá, J. L.; Ananias, D.; Carlos, L. D.; Rocha, J. *Angew. Chem., Int. Ed.* **2009**, *48*, 6476.
- (13) Ma, L.; Wu, C.-D.; Wanderley, M. M.; Lin, W. *Angew. Chem., Int. Ed.* **2010**, *49*, 8244.

- (14) Kumalah Robinson, S. A.; Mepin, M.-V. L.; Cairns, A. J.; Holman, K. T. *J. Am. Chem. Soc.* **2011**, *133*, 1634.
- (15) Wang, Z.; Cohen, S. M. *Chem. Soc. Rev.* **2009**, *38*, 1315.
- (16) Lu, H.; Zhang, X. P. *Chem. Soc. Rev.* **2011**, *40*, 1899.
- (17) Zimmerman, S. C.; Wendland, M. S.; Rakow, N. A.; Suslick, K. S. *Nat. Mater.* **2002**, *1*, 118.
- (18) Farha, O. F.; Shultz, A. M.; Sarjeant, A. A.; Nguyen, S. T.; Hupp, J. T. *J. Am. Chem. Soc.* **2011**, *133*, 5652.
- (19) Ono, K.; Yoshizawa, M.; Kato, T.; Watanabe, K.; Fujita, M. *Angew. Chem.* **2007**, *119*, 1835.
- (20) Larsen, R. W.; Wojtas, L.; Perman, J.; Musselman, R. L.; Zaworotko, M. J.; Vetromile, C. M. *J. Am. Chem. Soc.* **2011**, *133*, 10356.
- (21) Alkordi, M. H.; Liu, Y.; Larsen, R. W.; Eubank, J. F.; Eddaoudi, M. *J. Am. Chem. Soc.* **2008**, *130*, 12639.
- (22) Zhang, Z.; Zhang, L.; Wojtas, L.; Eddaoudi, M.; Zaworotko, M. J. *J. Am. Chem. Soc.* **2011**, DOI: 10.1021/ja208256u.
- (23) Das, S.; Kim, H.; Kim, K. *J. Am. Chem. Soc.* **2009**, *131*, 3814.
- (24) Prasad, T. K.; Hong, D. H.; Suh, M. P. *Chem.—Eur. J.* **2010**, *16*, 14043.
- (25) Zhao, J.; Mi, L.; Hu, J.; Hou, H.; Fan, Y. *J. Am. Chem. Soc.* **2008**, *130*, 15222.
- (26) Hambright, P. In *The Porphyrin Handbook*; Kadish, K. M., Smith, K. M., Guilard, R., Eds.; Academic Press: New York, 2000; Vol. 3, p 129.
- (27) Wong-Foy, A. G.; Lebel, O.; Matzger, A. J. *J. Am. Chem. Soc.* **2007**, *129*, 15740.
- (28) Ashby, C. I. H.; Paton, W. F.; Brown, T. L. *J. Am. Chem. Soc.* **1980**, *102*, 2990.
- (29) Allen, F. *Acta Crystallogr.* **2002**, *B58*, 380.
- (30) Spek, A. L. *Acta Crystallogr.* **1990**, *A46*, c34.
- (31) Berezin, D. B.; Shukhto, O. V.; Reshetyan, M. S. *Russ. J. Gen. Chem.* **2010**, *80*, 518.
- (32) Stults, B. R.; Marianelli, R. S.; Day, V. W. *Inorg. Chem.* **1979**, *18*, 1853.
- (33) Liu, C.-M.; Zhang, D.-Q.; Zhu, D.-B. *Inorg. Chem.* **2009**, *48*, 4980.
- (34) Eddaoudi, M.; Kim, J.; Vodak, D.; Sudik, A.; Wachter, J.; O'Keeffe, M.; Yaghi, O. M. *Proc. Natl. Acad. Sci. U.S.A.* **2002**, *99*, 4900.
- (35) Ma, S.; Sun, D.; Yuan, D.; Wang, X.-S.; Zhou, H.-C. *J. Am. Chem. Soc.* **2009**, *131*, 6445.
- (36) Rowsell, J. L. C.; Yaghi, O. M. *J. Am. Chem. Soc.* **2006**, *128*, 1304.
- (37) Zhou, W.; Wu, H.; Hartman, M. R.; Yildirim, T. *J. Phys. Chem. C* **2007**, *111*, 16131.
- (38) Latroche, M.; Surblé, S.; Serre, C.; Mellot-Draznieks, C.; Llewellyn, P. L.; Lee, J.-H.; Chang, J.-S.; Jhung, S. H.; Férey, G. *Angew. Chem., Int. Ed.* **2006**, *45*, 8227.
- (39) Sheldon, R. A. *Metalloporphyrins in Catalytic Oxidations*; Marcel Dekker: New York, 1994.